SCIENTIFIC REPORTS

OPEN

SUBJECT AREAS:
EXPERIMENTAL MODELS OF DISEASE
ALZHEIMER'S DISEASE
GENETIC VECTORS
PROTEASES

Received
5 December 2012

Accepted
4 March 2013

Published
18 March 2013

Correspondence and requests for materials should be addressed to N.I. (iwata-n@nagasaki-u.ac.jp) or T.C.S. (saido@brain.riken.jp)

Global brain delivery of neprilysin gene by intravascular administration of AAV vector in mice

Nobuhisa Iwata[1,2], Misaki Sekiguchi[1], Yoshino Hattori[2], Akane Takahashi[2], Masashi Asai[2], Bin Ji[3], Makoto Higuchi[3], Matthias Staufenbiel[4], Shin-ichi Muramatsu[5] & Takaomi C. Saido[1]

[1]Laboratory for Proteolytic Neuroscience, RIKEN Brain Science Institute, 2-1 Hirosawa, Wako-shi, Saitama 351-0198, Japan, [2]Laboratory of Molecular Biology and Biotechnology, Department of Molecular Medicinal Sciences, Graduate School of Biomedical Sciences, Nagasaki University, 1-14 Bunkyo-machi, Nagasaki-shi, Nagasaki 852-8521, Japan, [3]Molecular Imaging Center, National Institute of Radiological Sciences, 4-9-1 Anagawa, Inage-ku, Chiba-shi, Chiba 263-8555, Japan, [4]Novartis Institutes for Biomedical Research, 4002 Basel, Switzerland, [5]Division of Neurology, Department of Medicine, Jichi Medical University, 3311-1 Yakushiji, Shimotsuke-shi, Tochigi 329-0498, Japan.

Accumulation of amyloid-β peptide (Aβ) in the brain is closely associated with cognitive decline in Alzheimer's disease (AD). Stereotaxic infusion of neprilysin-encoding viral vectors into the hippocampus has been shown to decrease Aβ in AD-model mice, but more efficient and global delivery is necessary to treat the broadly distributed burden in AD. Here we developed an adeno-associated virus (AAV) vector capable of providing neuronal gene expression throughout the brains after peripheral administration. A single intracardiac administration of the vector carrying neprilysin gene in AD-model mice elevated neprilysin activity broadly in the brain, and reduced Aβ oligomers, with concurrent alleviation of abnormal learning and memory function and improvement of amyloid burden. The exogenous neprilysin was localized mainly in endosomes, thereby effectively excluding Aβ oligomers from the brain. AAV vector-mediated gene transfer may provide a therapeutic strategy for neurodegenerative diseases, where global transduction of a therapeutic gene into the brain is necessary.

Aggregation and deposition of amyloid-β peptide (Aβ) in the brain are triggering events of the long-term pathological cascade of Alzheimer's disease (AD), and are closely associated with the metabolic balance between Aβ anabolic and catabolic activities[1,2]. As almost all familial AD mutations cause an increase in the anabolism of a particular form of Aβ, $Aβ_{1-42}$, leading to Aβ deposition and accelerating AD pathology, a chronic reduction in the catabolic activity would also promote Aβ deposition[1,2]. Neprilysin (EC 3.4.24.11) is a rate-limiting peptidase involved in brain Aβ catabolism, as proven by *in vivo* experiments tracing the catabolism of radiolabeled Aβ in brain and by reverse genetics studies for candidate peptidases in mice[3,4]. Neprilysin gene-disruption caused a gene dosage-dependent elevation of endogenous Aβ levels in mouse brain, suggesting that a subtle but long-term reduction in neprilysin activity would contribute to AD development by promoting accumulation of Aβ[2].

Mounting evidence that expression levels of neprilysin are decreased in the hippocampus and cerebral cortex of AD patients from the early stages of disease development and also with aging in humans, as well as mice, suggests a close association of neprilysin with the etiology and pathogenesis of AD[2]. Indeed, reduced activity of neprilysin in mouse brain elevates the levels of highly toxic Aβ oligomers at the synapses, and leads to impaired hippocampal synaptic plasticity and cognitive function even before apparent amyloid deposition is observed in the brain[5]. Thus, a decline in neprilysin activity appears to be at least partly responsible for the memory-related symptoms of AD, and up-regulation of neprilysin is considered to be a promising strategy for therapy and prevention of AD.

Experimental gene therapy to transfer neprilysin gene into the brains of AD model mice has been reported, and for this purpose various kinds of recombinant viral vectors carrying wild-type neprilysin or its variants that are truncated at the transmembrane region and can be released to extracellular space have been utilized[6,7]. Viral vector-mediated delivery of neprilysin gene successfully retarded amyloid deposition in the brains of AD model mice[6,7]. Beneficial potential of gene therapy has also been shown in other neurodegenerative diseases, including Parkinson's disease (PD). Gene transfer of dopamine-synthesizing enzymes into the putamen alleviated motor

symptoms in PD patients[8,9]. However, infusion of viral vectors via stereotaxic surgery is not necessarily appropriate if the therapeutic gene should be delivered to broad areas of the brain.

In this study we have successfully developed a new gene delivery system by employing the combination of rAAV9 with a neuron-specific promoter, and we have shown that this system can provide functional gene expression throughout the brains of mice after intracardiac administration. The AAV vector can achieve comprehensive gene expression of neprilysin in the brain of young neprilysin-deficient mice, eventually decelerating Aβ accumulation and alleviating cognitive dysfunction based on a water maze test in aged APP transgenic (tg) mice. We show that the majority of the exogenous neprilysin is localized in late and early endosomes, where newly generated Aβ is concentrated, and this may be the reason why Aβ can be effectively excluded from the brain.

Results

Expression profile of neprilysin in the brain after AAV-mediated gene transfer. To deliver an AAV vector from circulating blood to the brain, we employed intracardiac administration, i.e., injection into the left ventricle of the heart, because this provides a direct route to the brain. To evaluate gene expression of neprilysin, we injected rAAV9 vectors that encode either an active or an inactive form of neprilysin in neprilysin-deficient mice[10] and examined the outcome by means of specific immunochemical staining for neprilysin. This staining generated specific signals of endogenous neprilysin in wild-type mice, but not in neprilysin-deficient mice without vector treatment (Fig. 1a,b). Expression of exogenous neprilysin after a single injection of rAAV9-NEP vector (4×10^{11} vector genome [v.g.]) into the left ventricle of the heart of neprilysin-deficient mice was spread over the limbic region on the neprilysin-null background (Fig. 1c,d), and presented a scattered distribution, but with locally intense signals. The total amount of exogenous neprilysin expression was dependent on amount of vector injected into the mice over a range of 0.5–4.0 $\times$ 10^{11} v.g., as far as we examined (data not shown). On the other hand, intracardiac administration of rAAV9-NEP vector did not cause prominent gene expression of neprilysin in heart, lung, kidney or liver (Supplementary Fig. 1).

Next, we examined the localization of neprilysin in the brain by confocal double immunostaining for neprilyin and several marker proteins, after the injection of rAAV9-NEP vector into neprilysin-deficient mice. Neprilysin was present in vesicular structures of NeuN-positive neurons (Fig. 2a–c), but not in glial fibrillary acidic protein (GFAP)-positive astrocytes (data not shown). In addition, we found that exogenous neprilysin is colocalized with late endosomal marker proteins Ras-related protein 7 (Rab7) (Fig. 2d–f) and Rab9 (Fig. 2g–i), and also in part with early endosomal markers Rab5 (Fig. 2j–l) and early endosome antigen 1 protein (EEA1) (Fig. 2m–o), but not with presynaptic markers SV2 (Fig. 2p–r) and syntaxin 1, secretory vesicle marker Rab3a, clathrin-coated vesicle marker clathrin heavy chain, somato-dendritic marker microtubule-associated protein 2 (MAP2), or postsynaptic marker PSD-95 (data not shown).

Functional expression of neprilysin. We investigated functional expression of neprilysin and subsequent reduction of Aβ levels in the brain. Four weeks after the single intracardiac injection of rAAV-NEP_{WT} vector into neprilysin-deficient mice, neprilysin activity in the limbic region including the neocortex and hippocampus was significantly increased compared to that after injection of rAAV-NEP_{MT} vector, although the increased level of neprilysin activity was less than 10% of the level observed in intact wild-type mice (Fig. 3). The injection of rAAV-NEP_{WT} vector into neprilysin-deficient mice significantly reduced Aβ40, Aβ42 and total Aβ levels in the limbic region compared to those in the mice injected with rAAV-NEP_{MT}. The partially compensated neprilysin activity was sufficient to achieve a 50% reduction of the elevated Aβ levels in the neprilysin-deficient mice.

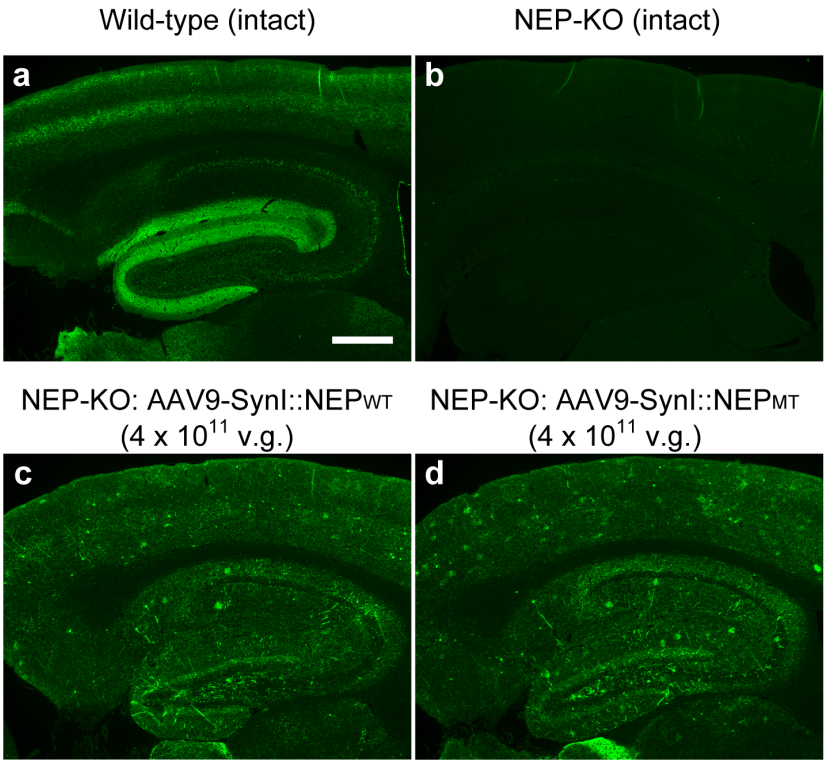

Figure 1 | Intracardiac injection of rAAV9 with SynI promoter leads to widespread gene transduction of neprilysin in the brain. Brain sections from intact wild-type mice (a), intact neprilysin-deficient mice (b), and neprilysin-deficient mice 14 days after intracardiac injection of 4×10^{11} genome vectors of rAAV9-SynI::NEP_{WT} (c) or rAAV9-SynI::NEP_{MT} (d). Scale bars, 200 μm.

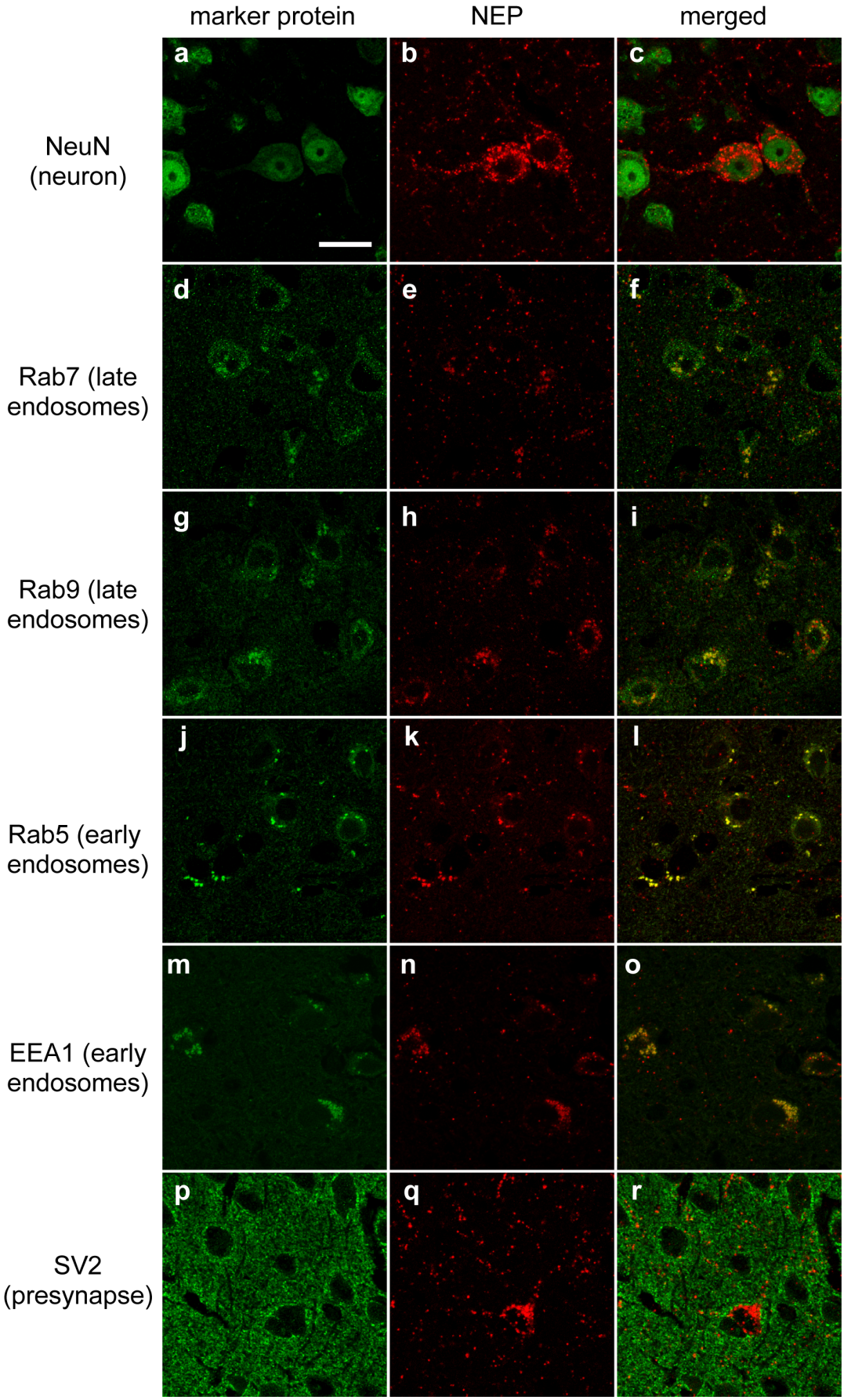

Figure 2 | Localization of the exogenous neprilysin in the brain. Brain sections from neprilysin-knockout mice 14 days after intracardiac injection of 4×10^{11} genome vectors of rAAV9-SynI::NEP_{WT}. Exogenous neprilysin was localized in NeuN-positive neurons (a–c), and was also observed in endosomes as confirmed by colocalization with Rab7 (d–f), Rab9 (g–i), Rab5 (j–l), EEA1 (m–o), and SV2 (p–r). Scale bars, 20 μm.

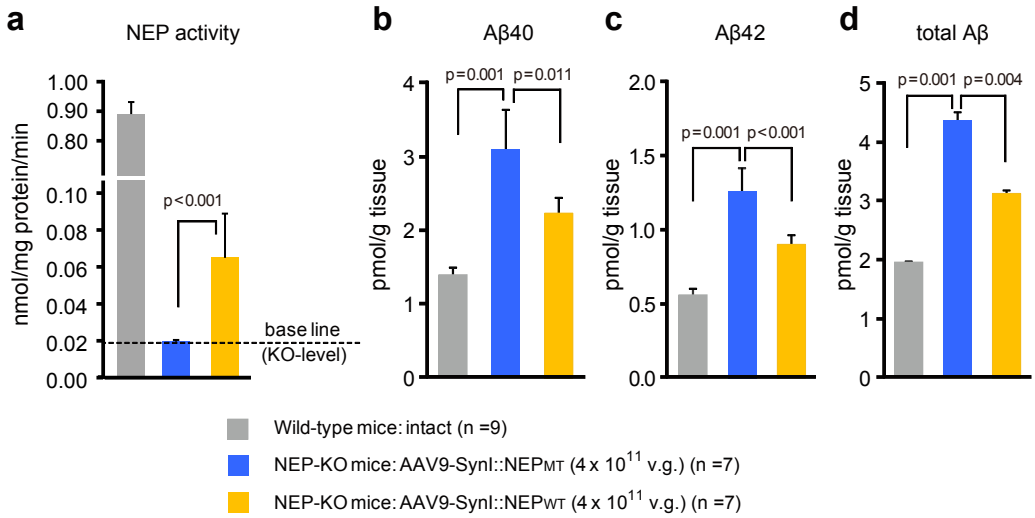

Figure 3 | Functional expression of NEP and Aβ levels in the limbic region after gene transfer. (a) Levels of neprilysin-dependent endopeptidase activity in the limbic regions of intact wild-type, rAAV9-SynI::NEP_{MT}- and rAAV-SynI::NEP_{WT}-injected NEP-KO mice 14 days after intracardiac injection. Data represent mean ± s.e.m. of 7–9 mice. (b–d) Levels of Aβ40, Aβ42 and total Aβs in the limbic regions after the gene transfer were determined by sandwich ELISA. A non-specific reaction of the ELISA system was excluded by subtracting values obtained in the brain tissue from APP-KO mice. Data represent mean ± s.e.m. of 7–9 mice.

Rescue of aged mutant APP tg mice from Aβ accumulation and subsequent impairment of memory and learning function. We next investigated the potential of intracardiac injection of rAAV9 vector to reverse the impaired memory and learning function in mutant APP tg mice (APP23)[11]. Since Aβ production in APP23 mice is about 10-fold higher than that of wild-type mice, a nearly 4-fold higher dose of vector was used than in the above-mentioned treatment of neprilysin-deficient mice. We examined reference memory as an indication of spatial memory and learning function, using a Morris water maze task. Under our experimental conditions, impairment of reference memory function of mutant APP tg mice was detected at the age of 15 months (Fig. 4a), and so we randomly divided mice of this age into two groups, which were given intracardiac administration of rAAV9-NEP_{MT} or rAAV-NEP_{WT}. Five months after the gene transfer, we re-examined their memory functions. The escape latency of rAAV9-NEP_{WT}-injected APP tg mice was significantly shorter than that of rAAV9-NEP_{MT}-injected mice ($*p < 0.05$), in which the escape latency was not shortened at all and the learning and memory function remained impaired (Fig. 4b). The cognitive function of the rAAV9-NEP_{WT}-injected APP tg mice was restored nearly to the level of intact wild-type mice. In addition, it is reported that anxiety-like behaviors affect performance in spatial learning tasks[12], and we cannot rule out the possibility that the effect of neprilysin gene transfer involved, at least in part, alleviation of anxiety-like behaviors that might have been exacerbated by the amyloid burden.

Next, we assessed plaque deposition and glial activation in the brains of rAAV9-injected APP tg mice by positron emission tomography (PET) with radioligands for amyloid (Pittsburgh Compound-B [^{11}C]PIB) and 18-kDa translocator protein (TSPO) ([^{11}C]Ac5216), respectively (Fig. 4c,d)[13,14]. Plaque deposition in both the hippocampus and neocortex was clearly reduced in the rAAV9-NEP_{WT}-injected mice compared to rAAV9-NEP_{MT}-injected mice ($*p < 0.05$). Mice treated with rAAV9-NEP_{WT} showed a tendency of enhanced TSPO upregulation, and the TSPO/amyloid burden ratio was significantly different between the two treatment groups ($*p < 0.05$). This observation is attributable to reinforcement of TSPO-positive, neuroprotective astrogliosis surrounding Aβ plaques[15]. Thus, *in vivo* assessments supported the potential effectiveness of gene therapy by intracardiac administration of rAAV9-NEP_{WT} in a pathological animal model.

Therapeutic effects of NEP gene transfer on Aβ pathologies in the brain. After PET imaging analysis (i.e., 6 months after the gene transfer), functional expression of neprilysin was estimated by measurement of enzyme activity using a standard fluorescent substrate, and amyloid deposition was assessed by immunohistochemical staining using specific antibodies against either the unmodified amino-terminus of Aβ, N1D, or the modified amino-terminus of Aβ, N3pE[16]. Neprilysin-dependent endopeptidase activity in both the hippocampus and the neocortex maintained a 1.5-fold increase in the rAAV9-NEP_{WT}-injected mice compared to that in rAAV9-NEP_{MT}-injected mice ($*p < 0.05$) (Fig. 5a), and both N1D- and N3pE-positive amyloid deposits were consistently and significantly decreased ($*p < 0.05$) (Fig. 5b,c).

We further investigated membrane-associated Aβ oligomers, which were extracted with Triton X-100 from the membrane fraction, using western blotting (Fig. 5d,e). Membrane-associated Aβs were detected as oligomers, consisting mainly of trimers/tetramers, followed by dimer, and with only a trace of monomer. The Aβ trimers/tetramers, which were not detected from non-tg (wild-type) mouse brain, were significantly decreased by the rAAV9-NEP_{WT} administration (20% reduction; $*p < 0.05$), compared to that in the rAAV9-NEP_{MT} group. According to the current hypothesis that Aβ oligomers are the primary molecules responsible for cognitive dysfunction, rather than Aβ fibrils[17–19], the reduction of Aβ oligomers following rAAV9-NEP_{WT} administration may contribute directly to the alleviation of abnormal spatial learning and memory function in aged mutant APP tg mice.

Discussion

Recombinant AAV vectors are among the most promising vehicles for gene delivery to the central nervous system. Stereotaxic infusion of AAV vector carrying neprilysin gene into the hippocampus has been shown to decrease Aβ in AD model mice[6,7]. However, when it was infused into the neocortex or hippocampal formation, expression of exogenous neprilysin and its effects on Aβ degradation were locally restricted[6,7]. Since the extent of the Aβ burden is broad in AD, a more efficient and widespread delivery technology is necessary. Among more than one hundred primate AAVs, AAV9 has gained much attention, showing high efficiency of gene transduction in neurons after intravenous administration in neonatal mice[20]. Here

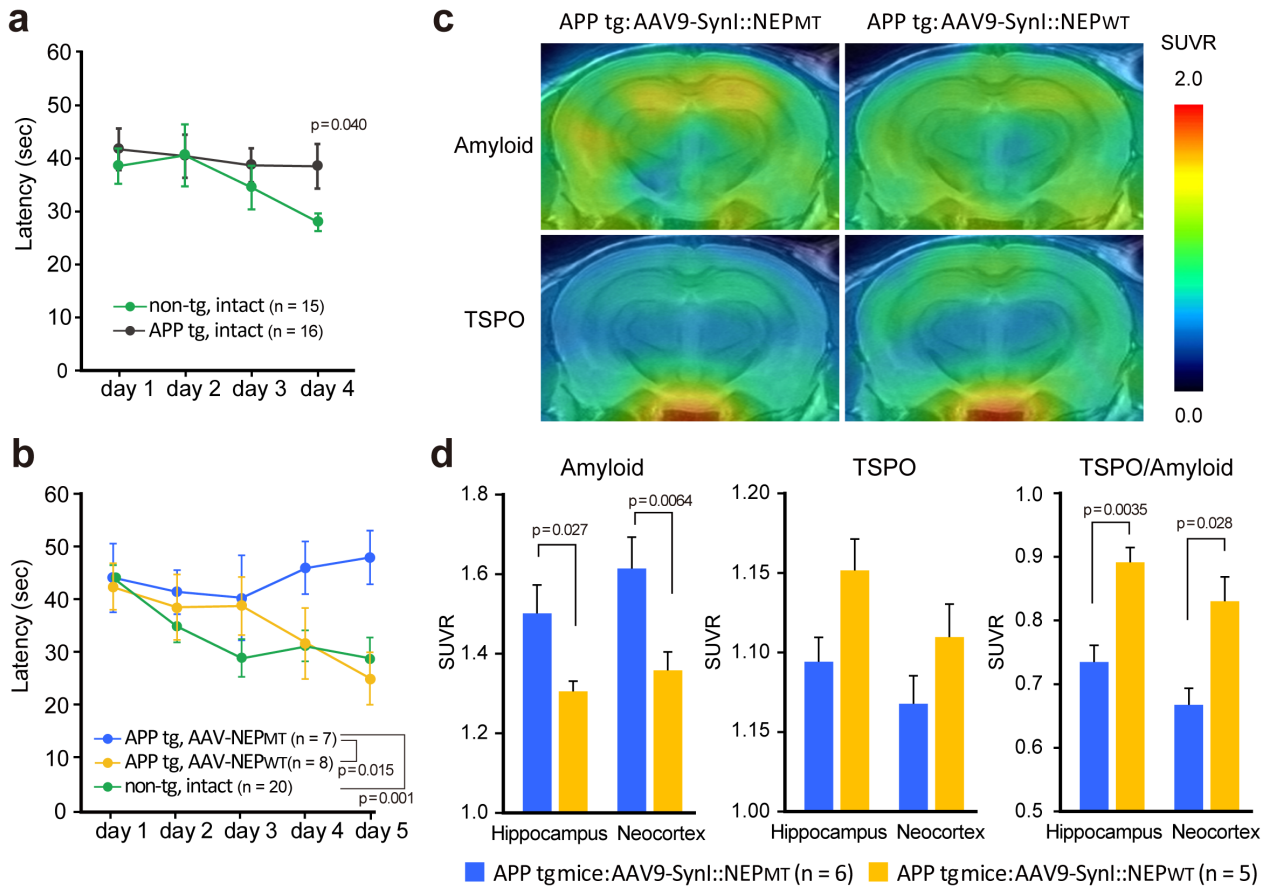

Figure 4 | NEP gene transfer ameliorated impaired spatial learning and memory function, amyloid burden, and modified glial activation in aged APP tg mice. Reference memory was examined using a water maze task. Escape latency in each block to the hidden platform during a 60-sec session was measured. (a) Impaired reference memory function of APP tg mice at the ages of 15 months was detected, and they were divided into two groups, followed by administration of AAV9-SynI::NEP_{MT} or AAV9-SynI::NEP_{WT} (1.5×10^{12} genome copies). Data represent mean ± s.e.m. (b) Five months after the gene transfer, their memory functions were re-examined. Two-way ANOVA showed a significant main effect of neprilysin gene transfer ($F_{(2,160)} = 6.287$; $p < 0.05$). *Post hoc* analysis revealed that the escape latency of rAAV9-SynI::NEP_{MT}-injected APP tg mice was significantly different from the other groups ($p < 0.05$). Data represent mean ± s.e.m. (c) Plaque deposition and glial activation in living brains of APP tg mice 5 months after injection of AAV9-SynI::NEP_{MT} and AAV9-SynI::NEP_{WT} assessed by PET with radioligands for amyloid ([^{11}C]PIB) (top) and TSPO ([^{11}C]Ac5216) (bottom). Amyloid and TSPO images are derived from the same individuals. Data represent mean ± s.e.m. (d) The levels were estimated as SUVRs. TSPO upregulation relative to amyloid abundance was also determined by calculating the quotient of the SUVRs for [^{11}C]Ac5216 and [^{11}C]PIB (right). The main effect of the treatment was significant on amyloid load ($F_{(1,12)} = 9.17$, $p < 0.05$) and TSPO-to-amyloid ratio ($F_{(1,10)} = 16.4$, $p < 0.01$) but insignificant on TSPO level ($F_{(1,10)} = 4.2$, $p > 0.05$) by repeated-measures 2-way ANOVA. The p values show significant differences between rAAV9-SynI::NEP_{WT} and rAAV-SynI::NEP_{WT}. Data represent mean ± s.e.m.

we showed that intracardiac administration of AAV9 can deliver neprilysin gene into broad areas of the adult mouse brain, and results in a marked and widespread reduction of Aβ levels. Although the mechanism by which AAV9 penetrates the blood-brain barrier (BBB) remains unknown, tyrosine mutation of the adeno-associated viral capsid protein may contribute to the enhanced expression levels of transgenes delivered by AAV[21].

It is noteworthy that a relatively small increase of neprilysin activity in the brain was sufficient to yield a significant reduction of Aβ, with subsequent alleviation of abnormal spatial learning and memory function. The exogenous neprilysin was abundantly present in late and early endosomes of neurons throughout the brain, including the neocortex and hippocampal formation. This localization appears to provide a rationale for the effective degradation of Aβ, as discussed below. It is considered that Aβ is generated in late endosomes, then is secreted from presynaptic terminals of neurons by neuronal activity-dependent exocytosis[22], and is temporally concentrated and may be oligomerized/aggregated. In addition, Walsh et al. reported that Aβ oligomerization occurred after generation of the peptide within specific intracellular vesicles including recycling endosomes[23], which could be modulated by Aβ *per se*[24], and the oligomers are subsequently secreted from the cell. This observation is supported by the fact that the mildly acidic environment (pH 5 ~ 6) in endosomes appears to promote Aβ oligomerization/aggregation[25]. After this event, Aβ or Aβ oligomers impair neuronal transmission via binding to *N*-methyl-D-aspartic acid (NMDA) or acetylcholine α7 nicotinic (α7nACh) receptors and prion protein[17–19]. Aβ/Aβ oligomers are diffused in the synaptic clefts after secretion, but they maintain a higher concentration in endosomal membrane, and may also be tethered in part at the plasma membrane. Although neprilysin is a neutral endopeptidase, its pH optimum is around 6.0[26], so neprilysin could degrade Aβ oligomers efficiently under the mildly acidic conditions in endosomes.

We succeeded in excluding membrane-associated Aβ oligomers from the brain by means of neprilysin gene transfer, ameliorating the impairment of spatial learning and memory function, although the contribution of a reduction in the total amount of amyloid deposition cannot be neglected. However, mounting evidence suggests that Aβ oligomers are highly neurotoxic[17–19] and may be more directly responsible for the pathological and symptomatic changes in AD,

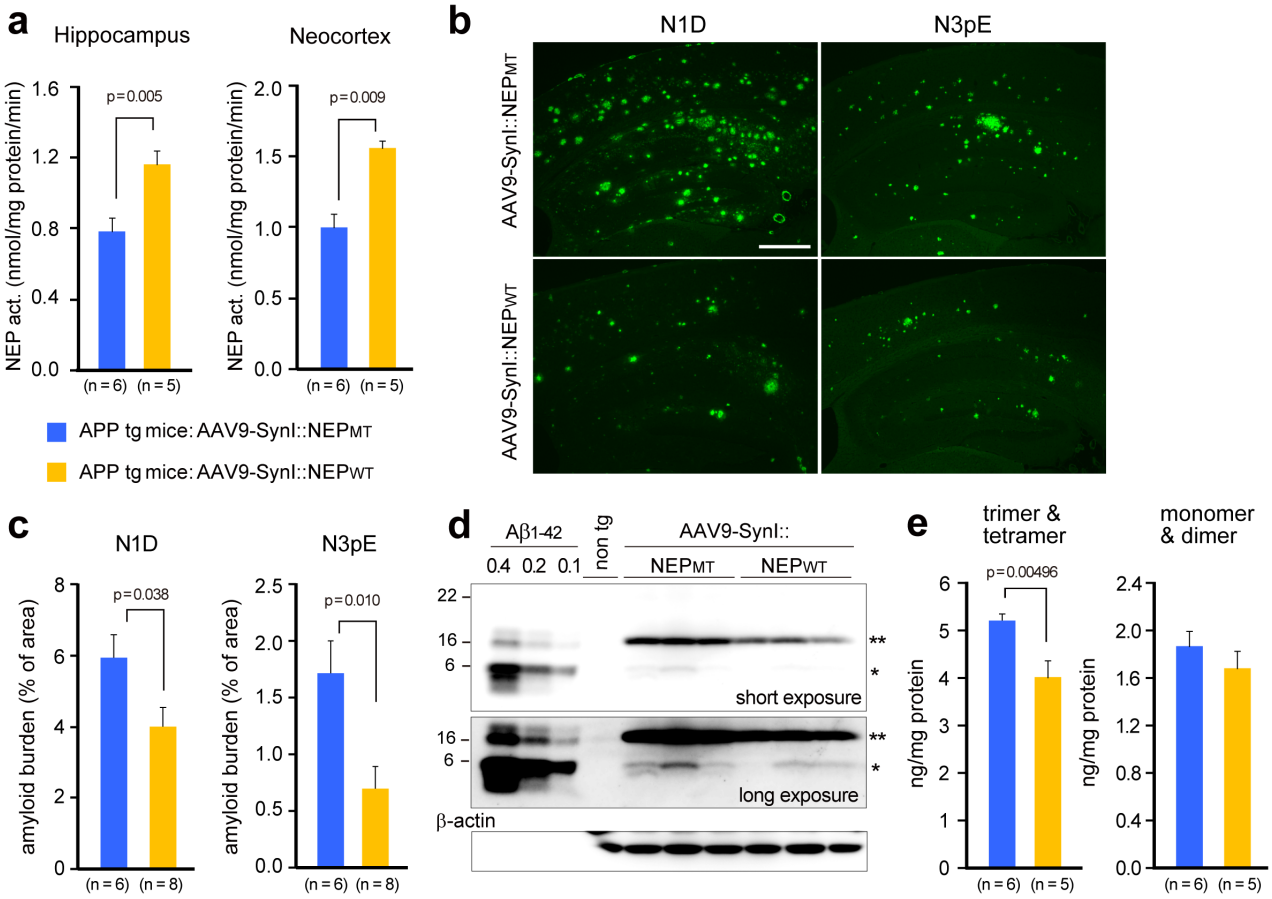

Figure 5 | Gene therapeutic effects of NEP gene transfer on Aβ pathologies in the brains. Seven months after the gene transfer into 15-month-old APP tg mice, brains were removed and analyzed biochemically and immunohistochemically. (a) NEP activities in the hippocampal formation and neocortex. (b) Amyloid burden. Brain sections were immunostained with N-terminal specific antibodies for Aβ (N1D and N3pE, mouse monoclonal). Scale bar, 500 μm. (c) Amyloid load is expressed as percent of the measured area. Data represent mean ± s.e.m. The *p* values show significant differences between rAAV9-SynI::NEP_{MT} and rAAV-SynI::NEP_{WT}. (d) A representative blot of Aβ and its oligomers. Triton X-100-extractable membrane fractions (20 μg protein) from the hippocampal formation of APP tg mice with rAAV9-NEP_{MT} or rAAV9-NEP_{WT} and non-transgenic (wild type) mice were subjected to western blot analyses using N-terminal specific antibody N1D (rabbit polyclonal). A single asterisk shows Aβ dimer, and a double asterisk shows trimer and tetramer. The blot was reprobed with anti-β-actin antibody. (e) Aβ oligomers in the blots were quantified by densitometry. Synthetic $Aβ_{1-42}$ (0.1, 0.2, 0.4 ng) run on the same gel as indicated in *d* was used for calibration within a linear range. The *p* values show significant differences between rAAV9-SynI::NEP_{MT} and rAAV-SynI::NEP_{WT}. Data represent mean ± s.e.m.

such as synaptic dysfunction and subsequent cognitive dysfunction[27]. This concept appears to be reinforced by a lesson from the failure of a clinical trial of Aβ vaccine[28], and thus supports the notion that reduction in neprilysin-sensitive and membrane-associated Aβ oligomers may be the key factor in the alleviation of cognitive impairment.

Aβ that accumulates and forms amyloid plaques in AD brain consists mostly of amino-terminally truncated and modified Aβ, AβN3pE[16], and this implies that Aβ secreted from neurons undergoes posttranslational modifications in the process of plaque formation. Although this fact has been known for decades, this specific form of Aβ, AβN3pE, has become of interest again since it was reported that PIB probe recognized AβN3pE with higher affinity than it did amino-terminally intact $Aβ_{1-42}$[13]. AβN3pE is more hydrophobic and more easily self-aggregated (250-fold) than $Aβ_{1-42}$[29], and is more resistant to proteolytic degradation (by 4-fold) (Iwata and Saido, unpublished data). Recently, it was reported that AβN3pE could be a seed for oligomerization/aggregation, and showed more potent neurotoxicity than AβN1D[30]. Schilling, et al. reported that administration of a synthetic inhibitor specific to glutaminyl cyclase (QC), which is involved in cyclization of the third glutamate residue of Aβ, reduced not only production of AβN3pE, but also the total amount of amyloid deposition, and it also alleviated cognitive impairment in AD-model mice (Tg2576)[31]. In this study, we found that the gene transfer abolished any increase in amyloid fibrils composed of AβN3pE, as well as amino-terminally intact Aβ, in the brains of aged APP tg mice (APP23). This result may be attributed to degradation of newly produced Aβ by exogenous neprilysin in endosomes, rather than direct degradation of AβN3pE. Because AβN3pE acquires proteolytic resistance once it is formed from $Aβ_{1-x}$, Aβ degradation in endosomes immediately after its production should be favorable for efficient degradation. This notion appears to be supported by the finding that we could not detect AβN3pE or its oligomeric forms in the membrane fraction (i.e., their concentrations were below the detection limit of western blot analysis)(data not shown).

Therapeutic intervention by neprilysin gene transfer could be monitored *in vivo* by using microPET with [^{11}C]PIB probe. TSPO is a marker protein in activated glias, such as astrocytes and microglias. Ji et al. reported that most TSPO-positive glial cells in aged APP tg mouse brains were astrocytes, which expressed glial cell line-derived neurotrophic factor at a high level[14,15], suggesting that TSPO-positive astrocytes may play neuroprotective roles in decelerated amyloid plaque formation and alleviation of abnormal spatial

learning and memory function. The precise mechanism through which up-regulation of neprilysin activates astrocytes in the brain remains unclear, but neprilysin-generated proteolytic fragments of substrate peptides may be involved in this process.

In conclusion, we have demonstrated that the new gene delivery system based on rAAV9 with a neuron-specific promoter can achieve functional gene expression throughout the brain, but not in peripheral tissues, after intracardiac administration. In our animal model, it could block Aβ accumulation and alleviate cognitive dysfunction based on a water maze test. Furthermore, the expression of neprilysin specifically in endosomes is considered to be advantageous for efficient degradation of Aβ oligomers.

Methods

Recombinant AAV vector production. The AAV vector plasmids contained an expression cassette, consisting of a mouse synapsin I promoter, followed by cDNA encoding neprilysin or its inactive mutant with E585V amino acid substitution, and a woodchuck hepatitis virus post-transcriptional regulatory element between the inverted terminal repeats of the AAV3 genome. The synthesized AAV9 vp cDNA sequence was identical to that previously described[21], except for the substitution of adenine with thymidine at position 1337, which introduced an amino acid change from tyrosine to phenylalanine at position 446[32]. The recombinant AAV vectors were produced by transient transfection of HEK293 cells with the vector plasmid, an AAV3 rep and AAV9 vp expression plasmid, and an adenoviral helper plasmid, pHelper (Agilent Technologies), as described previously[33]. The recombinant viruses were purified by isolation from two sequential continuous CsCl gradients, and the viral titers were determined by qRT-PCR. Before administration, rAAV vectors were diluted in phosphate-buffered saline to 0.5–15 $\times$ 10^{11} genome copies/100 μl.

Animals. All animal experiments were approved by the ethics committee at each institute (Nagasaki University, RIKEN Brain Science Institute, National Institute of Radiological Sciences, and Novartis Institutes for Biomedical Research), and performed in compliance with the institutional guidelines. Wild-type and neprilysin-deficient mice (7–9 months old)[10] were randomly assigned to rAAV-SynI::NEP_{WT} vector-injected and rAAV-SynI::NEP_{MT} vector-injected groups. One hundred μl of viral vector solution was injected slowly into circulating blood in the left ventricle of the heart of mice anesthetized with pentobarbital (50 mg/kg, ip) over a period of 1 min with a 0.5 ml syringe equipped with a 29-gauge needle. Male APP transgenic (APP23) mice[11] were randomly assigned to two groups at the age of 17 months, when overt abnormality in learning and memory function was observed in the water maze test. They were housed in plastic cages with food (CE2, Clea Japan, Tokyo, Japan) and water ad lib, and were maintained on a 12/12 h light-dark cycle (lights on at 09:00, off at 21:00).

Immunohistochemistry and quantitative evaluation. One week after amyloid imaging of the vector-injected APP tg mice, the mouse brains were fixed by transcardial perfusion with phosphate-buffered 4% paraformaldehyde and embedded in paraffin. Four-μm-thick sections were mounted onto aminopropyltriethoxysilane-coated glass slides. The brain sections were immunostained using mouse monoclonal anti-neprilysin antibody or mouse monoclonal anti-Aβ antibody against either unmodified amino-terminus of Aβ, N1D, or modified amino-terminus of Aβ, N3pE, and visualized with AlexaFluor 488-conjugated secondary antibody. The sections were observed with a fluorescence microscope, BZ-9000 (Keyence, Osaka, Japan), using a $\times$2 or a $\times$4 objective with 1.3$\times$ digital zoom, and digital images were captured with a digital microscope camera (Keyence) and saved as digitized tagged-image format files to retain maximum resolution. The density of immunoreactive Aβ deposits in the hippocampal formation and neocortex was measured using image analysis software, MetaMorph, ver. 7.7 (Universal Imaging Corporation, Downington, PA), by an investigator blinded as to sample identity. To reduce the variance among tissue sections, we used the average of data from 4 sections per mouse as an individual value.

In addition to Aβ immunolabeling, multiple immunofluorescence staining was performed as described previously[34]. For double staining of neprilysin and cell or organelle marker proteins (NeuN, GFAP, MAP2, tau, syntaxin-1, SV2A, VAMP-1, PSD95, Rab3a, Rab5, Rab7, Rab9, Clathrin, EEA1, Syntaxin-6), brain sections from neprilysin-deficient mice administered with rAAV9-SynI::NEP were first immunostained using a fluorescence-direct TSA method (Texas-Red-conjugated streptoavidin) combined with anti-neprilysin mouse monoclonal antibody, and then with rabbit polyclonal anti-marker protein antibodies and AlexaFluor 488-conjugated secondary antibody or EnVision plus system HRP-labeled polymer anti-rabbit antibody. The sections were observed under an Axio observer Z1 inverted microscope incorporating a confocal laser scanning system LSM710 with argon, helium/neon (G) and helium/neon (R) lasers (Carl Zeiss Japan, Tokyo, Japan). Alexa 488 and Texas-red were excited with 488 nm and 543 nm laser beams, and observed through 510–530 nm, and 560–600 nm band pass emission filters, respectively. All of the single images were acquired by quintuple scans with ZEN2008, ver. 5.0 software (Carl Zeiss Japan) using a $\times$63 oil immersion objective, then merged and saved as digitized tagged-image format files to retain maximum resolution.

Behavioral analysis. Five months after the injection of rAAV vector into APP tg mice, the Morris water maze test was conducted as previously reported[5], with minor modifications. Further details are available in the online supplementary information.

***In vivo* imaging of amyloid and glial activation.** Positron emission tomographic (PET) scans were conducted for APP tg mice at 20 months of ageas described elsewhere[13,14] with a microPET Focus 220 animal scanner (Siemens Medical Solutions USA, Knoxville, TN) designed for small animals, which provides 95 transaxial slices 0.815 mm (center-to-center) apart, a 19.0-cm transaxial field of view (FOV) and a 7.6-cm axial FOV[35]. Prior to the scans, the mice were anesthetized with 1.5% (v/v) isoflurane. Further details are available in the online supplementary information.

Assay of neprilysin-dependent neutral endopeptidase activity. Hippocampal formations and cerebral cortices were homogenized in five volumes (w/v) of 50 mM Tris-HCl buffer (pH 7.6) containing 150 mM NaCl, protease inhibitor cocktail (EDTA-free Complete™, Roche Diagnostics, Indianapolis, IN) supplemented with 0.7 μg/ml pepstatin A (4397, Peptide Institute, Osaka, Japan) with a Potter-Elvehjem-type grinder (Wheaton, Millville, NJ). The homogenates were centrifuged at 70,000 rpm and 4°C for 29 min using an Optima TL ultracentrifuge and a TLA100.4 rotor (Beckman, Palo Alto, CA). The pellet was solubilized with the above buffer containing 1% Triton X-100 (membrane fraction). NEP-dependent neutral endopeptidase activity in the membrane fraction was fluorometrically assayed using an indirect coupled enzyme assay method. The standard assay mixture consisted of 4–6 μg of membrane fraction, 0.1 mM succinyl-Ala-Ala-Phe-AMC (I-1315; Bachem, Bubendorf, Switzerland) as a substrate, and 100 mM MES buffer (pH 6.5) in a total volume of 50 μL. The reaction was initiated by addition of substrate to the assay mixture, and performed for 1 h at 37°C. To the reaction mixture was then added 2.5 μL of a solution containing 0.1 mg (0.4 units equivalent)/mL leucine aminopeptidase (L-5006; Sigma, St Louis, MO) and 0.2 mM phosphoramidon (4082; Peptide Institute), followed by further incubation for 30 min at 37°C to remove the phenylalanine residue from Phe-AMC generated by neutral endopeptidase-catalyzed digestion. The intensity of the liberated 7-amino-4-methylcoumarin was measured with excitation at 390 nm and emission at 460 nm on a 96-well half-area-black half-well plate using a microplate spectrometer Infinite M-1000 (Tecan Group Ltd., Männedorf, Switzerland). The NEP-dependent neutral endopeptidase activity was determined, based on the decrease in rate of digestion caused by 10 μM thiorphan (T-6031; Sigma), a specific inhibitor of NEP[36]. Protein concentrations were determined using a bicinchoninic acid protein assay kit (Pierce, Rockford, IL).

Aβ quantitation. The cerebral cortices and hippocampi were processed according to the method reported previously[6]. The amounts of Aβx-40 and Aβx-42 in each fraction were determined by sandwich ELISA (Wako, Osaka, Japan).

Western blotting. The Triton X-100-extractable membrane fraction of hippocampi was used for analysing levels of Aβ oligomers and monomers. Protein concentrations were determined using a BCA protein assay kit (Pierce, Rockford, IL). An equivalent amount of protein from hippocampus of each animal was mixed with a 2$\times$ sample buffer without a reducing agent, separated by 5–20% gradient SDS-polyacrylamide gel electrophoresis and transferred electrophoretically to a 0.22 μm nitrocellulose membrane (Protoran®, Whatman GmbH, Dassel, Germany). The membrane was boiled in PBS for 3 min to achieve high sensitivity. The blot was probed with anti-rabbit polyclonal antibody against either unmodified amino-terminus of Aβ, N1D (1 μg/ml) or modified amino-terminus of Aβ, N3pE (1 μg/ml)[16], followed by HRP-conjugated anti-rabbit IgG (GE Healthcare, Tokyo). Immunoreactive bands on the membrane were visualized with an enhanced chemiluminescence kit (GE Healthcare), and the band intensities were determined with a densitometer, LAS4000 (Fuji Photo Film, Tokyo, Japan) using Science Lab 97 Image Gauge software (ver. 3.0.1; Fuji Photo Film). Immunoreactive protein content in each sample was calculated based on a standard curve constructed with synthesized Aβ (Peptide Institute, Osaka, Japan). Each set of experiments was repeated at least two times. The blots were reprobed with anti-β-actin (AC-15, Sigma) antibody to confirm that equal amounts of total protein had been extracted.

Statistical analysis. All data were expressed as means $\pm$ s.e.m. For comparisons of the means between two groups, statistical analysis was performed by applying Student's *t* test after confirming equality of variances of the groups. If the variances were unequal, Mann-Whitney *U*-test was performed (SigmaPlot software, ver.12.3, Systat Software Inc., San Jose, CA). Comparisons of the means among more than three groups were done by a one-way or two-way analysis of variance (ANOVA) or repeated-measures ANOVA followed by a *post-hoc* test (SigmaPlot software). *P* values of less than 0.05 were considered to be significant.

Details for antibodies used in this study are available in the online supplementary information.

1. Hardy, J. & Selkoe, D. J. The amyloid hypothesis of Alzheimer's disease: progress and problems on the road to therapeutics. *Science* **297**, 353–356 (2002).
2. Iwata, N., Higuchi, M. & Saido, T. C. Metabolism of amyloid-β peptide and Alzheimer's disease. *Pharmacol. Ther.* **108**, 129–148 (2005).

3. Iwata, N. *et al*. Identification of the major $A\beta_{1-42}$-degrading catabolic pathway in brain parenchyma: suppression leads to biochemical and pathological deposition. *Nat. Med.* **6**, 143–150 (2000).
4. Iwata, N. *et al*. Metabolic regulation of brain Aβ by neprilysin. *Science* **292**, 1550–1552 (2001).
5. Huang, S. M. *et al*. Neprilysin-sensitive synapse-associated amyloid-β peptide oligomers impair neuronal plasticity and cognitive function. *J. Biol. Chem.* **281**, 17941–17951 (2006).
6. Iwata, N. *et al*. Presynaptic localization of neprilysin contributes to efficient clearance of amyloid-β peptide in mouse brain. *J. Neurosci.* **24**, 991–998 (2004).
7. Nilsson, P. *et al*. Gene therapy in Alzheimer's disease - potential for disease modification. *J. Cell. Mol. Med.* **14**, 741–757 (2010).
8. Muramatsu, S. *et al*. A phase I study of aromatic L-amino acid decarboxylase gene therapy for Parkinson's disease. *Mol. Ther.* **18**, 1731–1735 (2010).
9. Christine, C. W. *et al*. Safety and tolerability of putaminal AADC gene therapy for Parkinson disease. *Neurology* **73**, 1662–1669 (2009).
10. Lu, B. *et al*. Neutral endopeptidase modulation of septic shock. *J. Exp. Med.* **181**, 2271–2275 (1995).
11. Sturchler-Pierrat, C. *et al*. Two amyloid precursor protein transgenic mouse models with Alzheimer disease–like pathology. *Proc. Natl. Acad. Sci. USA* **94**, 13287–13292 (1997).
12. Miyakawa, T. *et al*. Neurogranin null mutant mice display performance deficits on spatial learning tasks with anxiety related components. *Hippocampus* **11**, 763–775 (2001).
13. Maeda, J. *et al*. Longitudinal, quantitative assessment of amyloid, neuroinflammation, and anti-amyloid treatment in a living mouse model of Alzheimer's disease enabled by positron emission tomography. *J. Neurosci.* **27**, 10957–10968 (2007).
14. Maeda, J. *et al*. *In vivo* positron emission tomographic imaging of glial responses to amyloid-β and tau pathologies in mouse models of Alzheimer's disease and related disorders. *J. Neurosci.* **31**, 4720–4730 (2011).
15. Ji, B. *et al*. Imaging of peripheral benzodiazepine receptor expression as biomarkers of detrimental versus beneficial glial responses in mouse models of Alzheimer's and other CNS pathologies. *J. Neurosci.* **28**, 12255–12267 (2008).
16. Saido, T. C. *et al*. Dominant and differential deposition of distinct β-amyloid peptide species, $A\beta_{N3(pE)}$, in senile plaques. *Neuron* **14**, 457–466 (1995).
17. Haass, C. & Selkoe, D. J. Soluble protein oligomers in neurodegeneration: lessons from the Alzheimer's amyloid β-peptide. *Nat. Rev. Mol. Cell. Biol.* **8**, 101–112 (2007).
18. Benilova, I., Karran, E. & De Strooper, B. The toxic Aβ oligomer and Alzheimer's disease: an emperor in need of clothes. *Nat. Neurosci.* **15**, 349–357 (2012).
19. Larson, M. E. & Lesné, S. E. Soluble Aβ oligomer production and toxicity. *J. Neurochem.* **120 Suppl 1**, 125–139 (2012).
20. Foust, K. D. *et al*. Intravascular AAV9 preferentially targets neonatal neurons and adult astrocytes. *Nat. Biotechnol.* **27**, 59–65 (2009).
21. Petrs-Silva, H. *et al*. Novel properties of tyrosine-mutant AAV2 vectors in the mouse retina. *Mol. Ther.* **19**, 293–301 (2011).
22. Cirrito, J. R. *et al*. Endocytosis is required for synaptic activity-dependent release of amyloid-β *in vivo*. *Neuron* **58**, 42–51 (2008).
23. Walsh, D. M. *et al*. Naturally secreted oligomers of amyloid β protein potently inhibit hippocampal long-term potentiation *in vivo*. *Nature* **416**, 535–539 (2002).
24. Abramov, E. *et al*. Amyloid-β as a positive endogenous regulator of release probability at hippocampal synapses. *Nat. Neurosci.* **12**, 1567–1576 (2009).
25. Bharadwaj, P. R. *et al*. Aβ aggregation and possible implications in Alzheimer's disease pathogenesis. *J. Cell. Mol. Med.* **13**, 412–421 (2009).
26. Kerr, M. A. & Kenny, A. J. The molecular weight and properties of a neutral metallo-endopeptidase from rabbit kidney brush border. *Biochem. J.* **137**, 489–495 (1974).
27. Selkoe, D. J. Alzheimer's disease is a synaptic failure. *Science* **298**, 789–791 (2002).
28. Holmes, C. *et al*. Long-term effects of Aβ42 immunisation in Alzheimer's disease: follow-up of a randomised, placebo-controlled phase I trial. *Lancet* **372**, 216–223 (2008).
29. Schilling, S. *et al*. On the seeding and oligomerization of pGlu-amyloid peptides (*in vitro*). *Biochemistry* **45**, 12393–12399 (2006).
30. Nussbaum, J. M. *et al*. Prion-like behaviour and tau-dependent cytotoxicity of pyroglutamylated amyloid-β. *Nature* **485**, 651–655 (2012).
31. Schilling, S. *et al*. Glutaminyl cyclase inhibition attenuates pyroglutamate Aβ and Alzheimer's disease-like pathology. *Nat. Med.* **14**, 1106–1111 (2008).
32. Gao, G. *et al*. Clades of adeno-associated viruses are widely disseminated in human tissues. *J. Virol.* **78**, 6381–6388 (2004).
33. Li, X. G. *et al*. Viral-mediated temporally controlled dopamine production in a rat model of Parkinson disease. *Mol. Ther.* **13**, 160–166 (2006).
34. Fukami, S. *et al*. Aβ-degrading endopeptidase, neprilysin, in mouse brain: synaptic and axonal localization inversely correlating with Aβ pathology. *Neurosci. Res.* **43**, 39–56 (2002).
35. Tai, Y. C. *et al*. Performance evaluation of the microPET focus: a third generation microPET scanner dedicated to animal imaging. *J. Nucl. Med.* **46**, 455–463 (2005).
36. Roques, B. P. *et al*. The enkephalinase inhibitor thiorphan shows antinociceptive activity in mice. *Nature* **288**, 286–288 (1980).

Acknowledgements

The authors thank Naomi Takino, Hitomi Miyauchi, Keiko Ayabe (Jichi Med. Univ.), Kaori Watanabe (Nagasaki Univ.) and Ryo Fujioka (Riken) for technical assistance. We also thank Dr. Craig Gerard (Harvard Medical School) for providing neprilysin-knockout mice. This work was supported in part by a research grant from RIKEN BSI, a grant-in-aid for scientific research from JSPS (23590473), a grant-in-aid via the research committee on CNS degenerative diseases from the MHLW, and grants-in-aid for the Japan Advanced Molecular Imaging Program and for scientific research on innovative areas (Synapse Neurocircuit Pathology) from the MEXT.

Author contributions

S.M. designed and prepared the AAV vectors; N.I. and M. Sekiguchi performed the in vivo experiments, N.I., Y.H., A.T., M.A. performed biochemical and histochemical analyses; B.J. and M.H. performed the PET imaging analysis; M. Staufenbiel provided APP tg mice; N.I., S.M., M.H., M. Staufenbiel and T.C.S. designed the experimental plan and wrote the manuscript.

Additional information

Supplementary information accompanies this paper at http://www.nature.com/scientificreports

Competing financial interests: The authors declare no competing financial interests.

How to cite this article: Iwata, N. *et al*. Global brain delivery of neprilysin gene by intravascular administration of AAV vector in mice. *Sci. Rep.* **3**, 1472; DOI:10.1038/srep01472 (2013).